Nonequilibrium Concentration Fluctuations in Binary Liquid Systems Induced by the Soret Effect

Jan V. Sengers[1] and José M. Ortiz de Zárate[2]

[1] Institute for Physical Science and Technology and Department of Chemical Engineering, University of Maryland, College Park, MD 20742, USA
[2] Departamento de Física Aplicada 1, Facultad de Ciencias Físicas, Universidad Complutense, E-28040 Madrid, Spain

Abstract. When a binary liquid system is brought into a stationary thermal nonequilibrium state by the imposition of a temperature gradient, the Soret effect induces long-range concentration fluctuations even in the absence of any convective instability. The physical origin of the nonequilibrium concentration fluctuations is elucidated and it is shown how the intensity of these concentration fluctuations can be derived from the linearized random Boussinesq equations. Relevant experimental information is also discussed.

1 Introduction

In this chapter we consider a binary liquid system located between two horizontal plates with two different but constant temperatures. A temperature gradient in a liquid mixture induces a concentration gradient through the Soret effect [1–5]. Many studies reported in the literature have been concerned with the effect of the Soret-induced concentration gradients on the convective Rayleigh-Bénard instability [6–11]. However, it turns out that there are also interesting fluctuation phenomena present, when the liquid mixture is in a hydrodynamically quiescent stable state, far away from any convective instability. It is the purpose of the present chapter to review the origin and the nature of concentration fluctuations in a binary liquid in stable convection-free thermal nonequilibrium states.

About 50 years ago a procedure for dealing with nonequilibrium phenomena in fluids was proposed by Bogoliubov [12,13]. It was based on a postulate that a fluid in a nonequilibrium state would proceed to thermodynamic equilibrium in two distinct stages: first a microscopic kinetic stage with a time scale of the order of the interval between successive molecular collisions, which for liquids is of the same order as the duration of the molecular collisions, after which local equilibrium is established; second a macroscopic stage during which the fluid evolves in accordance with the hydrodynamic equations. Implicit in this postulate is the idea that no long-range dynamic correlations would be present in a fluid of molecules with short-range forces, unless the system would be near an incipient thermodynamic or hydrodynamic instability.

The subsequent 25 years in the history of nonequilibrium statistical mechanics have revealed a basic flaw in this picture. In evaluating the randomizing

W. Köhler and S. Wiegand (Eds.): LNP 584, pp. 121–145, 2002.

nature of molecular collisions one must make a distinction between quantities like mass, momentum and energy that are conserved in a binary collision on the one hand and nonconserved quantities on the other hand. The fast modes associated with nonconserved quantities do indeed decay during a short kinetic stage, but the slow modes associated with the conserved quantities persist well beyond the time between successive collisions and a coupling between these modes can result in long-range (mesoscopic) dynamic correlations [14]. The classical picture of short-range dynamic correlations first appeared to be inadequate in fluids near the critical point when experiments [15] could no longer be explained by the Van Hove theory of the critical slowing down of the fluctuations which was based on strictly thermodynamic considerations; this observation led to the development of the mode-coupling theory of critical dynamics [16–19]. Some time later it turned out that the same mode-coupling theory could also account for the presence of long-time tails in the Green-Kubo correlation functions that were originally noticed from computer simulations of molecular dynamics [20–22].

Around 1980 it became evident that the mode-coupling theory would also predict the existence of long-range temperature and viscous fluctuations in fluids that are kept in stationary nonequilibrium states [23]. Specifically, Kirkpatrick et al. were the first to derive the appropriate expressions for the temperature and the viscous fluctuations in a one-component fluid subjected to a stationary temperature gradient [24]. Subsequently, others have recovered the same expressions on the basis of Landau's fluctuating hydrodynamics [25–31]. Physically, the presence of a temperature gradient ∇T leads to nonequilibrium fluctuations because the stationary temperature gradient causes a coupling between the component of the velocity fluctuations parallel to the gradient and the temperature fluctuations. Velocity fluctuations parallel to the gradient are probing regions with different local equilibrium temperatures, thus causing a nonequilibrium contribution to the temperature fluctuations. Since both the temperature and the viscous (transverse velocity) fluctuations do not propagate, but decay diffusively, the nonequilibrium contributions cannot depend on whether the temperature gradient is in the positive or negative direction and, hence, they depend on the square of the temperature gradient. Moreover, each mode contributes a factor q^{-2}, so that the intensity of the nonequilibrium fluctuations becomes inversely proportional to the fourth power of the wave number q of the fluctuations. The dependence of the intensity of the nonequilibrium fluctuations on $(\nabla T)^2$ and on q^{-4} has been confirmed by light-scattering experiments [32–35]. An algebraic divergence of the nonequilibrium fluctuations as a function of the wave number q is now believed to be a general feature of fluctuations in fluids in stationary nonequilibrium states [14,36,37].

The ultimate divergence of the intensity of nonequilibrium fluctuations for small wave numbers, i.e., for large wavelengths, will be prevented by gravity and finite-size effects. Specifically, for very small wave numbers the dependence of the nonequilibrium fluctuations on q is suppressed by the presence of gravity, as predicted theoretically by Segrè et al. [38] and confirmed experimentally by

Vailati and Giglio [39,40], and also modified by finite-size effects, as evaluated by Ortiz de Zárate et al. [41,42].

In the case of a liquid mixture, a temperature gradient ∇T is accompanied by a concentration gradient ∇c through the Soret effect as mentioned earlier. Just as a temperature gradient causes a coupling between the temperature fluctuations with wave vector $\boldsymbol{q}$ perpendicular to the temperature gradient and the transverse-velocity fluctuations in the direction of the temperature gradient, so will a concentration gradient cause a coupling between the concentration fluctuations with wave vector $\boldsymbol{q}$ perpendicular to the concentration gradient and the transverse-velocity fluctuations in the direction of the concentration gradient. Hence, in a liquid mixture subjected to a temperature gradient not only nonequilibrium temperature and viscous fluctuations will be present, but also nonequilibrium concentration fluctuations as first pointed out by Law and Nieuwoudt [43,44], and as also analyzed by Velasco and García Colín [45] and by Segrè and Sengers [46]. The intensity of the nonequilibrium concentration fluctuations should be proportional to the square of the concentration gradient ∇c and again inversely proportional to the fourth power of the wave number q. At very small q, the nonequilibrium concentration fluctuations will again be modified by gravity effects [39,46] and by finite-size effects [47].

The case of nonequilibrium concentration fluctuations in a colloidal suspension in the presence of a concentration gradient has been considered by Schmitz [48]. Vailati and Giglio [49] have extended the theory to treating the effect of time-dependent concentration profiles on the structure factor of a binary liquid.

The complete expressions for the contributions from the nonequilibrium viscous fluctuations, temperature fluctuations and concentration fluctuations to the dynamic structure factor of binary fluids are rather complicated [43,44,46]. However, in the case of (nearly) incompressible liquid mixtures a number of simplifying approximations can be made. First of all, as documented elsewhere [34,46,50], to a good approximation the decay rates of the viscous fluctuations, the temperature fluctuations and the concentration fluctuations can be directly identified with νq^2, $D_{\mathrm{th}} q^2$, and Dq^2, respectively, where ν is the kinematic viscosity, D_{th} the thermal diffusivity and D the (mass) diffusion coefficient. Furthermore, the diffusion coefficient D is much smaller than the kinematic viscosity ν and the thermal diffusivity D_{th}. Thus, the viscous and thermal fluctuations have in practice decayed at the times that the concentration fluctuations are still important. Moreover, because of the dependence of the refractive index on the concentration, the intensity of light scattered by the concentration fluctuations is usually appreciably larger than that from the viscous or the temperature fluctuations. Hence, in many cases one can readily determine the concentration fluctuations with Rayleigh scattering independently from the much faster decaying viscous and temperature fluctuations [34,35,50,51].

In this chapter we shall present a simple derivation of the intensity of the nonequilibrium concentration fluctuations and their contribution to Rayleigh scattering. Instead of considering the full (complicated) structure factor [43,46] and then make a series of simplifying approximations, we shall show how the intensity of the nonequilibrium concentration fluctuations can be readily derived from the same linearized random Boussinesq equations commonly used for studying the convective instability in binary fluids [6–11], including the bouyancy term and, thus, the effects of gravity. Specifically, we shall adopt an approximation to the Boussinesq equations proposed by Velarde and Schechter to simplify the study of the linear stability problem [52]. Therefore, instead of using the full hydrodynamic equations, making a complicated derivation of the structure factor and, then, simplify it by retaining only the experimentally important terms, we shall make the simplification *a priori*, by adopting a set of approximate Boussinesq equations supplemented with random noise terms in accordance with fluctuating hydrodynamics [53,54]. The advantage of this approach is that the calculation of the structure factor associated with the nonequilibrium concentration fluctuations becomes simple and straightforward, while elucidating the physical origin of the nonequilibrium fluctuations. This simplified approach facilitates not only the inclusion of gravity effects to be discussed in this chapter, but also the incorporation of finite-size effects on the nonequilibrium concentration fluctuations to be considered in a future publication [47].

2 Theory

We consider a horizontal layer of a binary liquid subjected to a stationary temperature gradient to be designated as ∇T_0, which as a result of the Soret effect is accompanied by a stationary concentration gradient to be designated as ∇c_0. The temperature gradient is assumed to act in the vertical Z-direction, while being uniform in the X and Y directions. The thermal conductivity is assumed to vary weakly with temperature so that $\nabla T_0 = dT_0/dz$ and $\nabla c_0 = dc_0/dz$ are (scalar) constants independent of the position in the liquid layer. The relationship between the temperature gradient ∇T_0 and the resulting concentration gradient ∇c_0 is given by:

$$\nabla c_0 = -c\,(1-c)\;S_T\;\nabla T_0, \tag{1}$$

where c is the (average) concentration expressed as weight fraction (w/w) of component 1 of the mixture. Equation (1) defines the Soret coefficient S_T of component 1 in component 2. Hence, component 1 is considered the solute and component 2 the solvent. For isotropic mixtures S_T is a scalar quantity and the induced concentration gradient is parallel to the imposed temperature gradient, but depending on the sign of S_T can have the same or the opposite direction. When S_T is positive, concentration and temperature gradients have opposite directions, with component 1 migrating to the colder region. When S_T is negative, concentration and temperature gradients have the same direction, with component 1 migrating to the warmer region. If c were to represent the concentration of component 2, then (1) would define the Soret coefficient S_T of component 2 in component 1. For a given mixture mass conservation implies that when S_T of component 1 in component 2 is positive, the S_T of component 2 in component

1 must be negative and *vice versa*. In this chapter we adopt the convention that c designates the concentration of component 1.

Let ρ be the density of the liquid layer, $\alpha = -\rho^{-1}\ (\partial\rho/\partial T)_c$ the thermal expansion coefficient and $\beta = \rho^{-1}\ (\partial\rho/\partial c)_T$ the concentration expansion coefficient. Since the liquid mixture is assumed to be (nearly) incompressible, the pressure is not a relevant physical variable. We note that β is positive when component 1 is the heavier component and β is negative when component 1 is the lighter component. A dimensionless separation ratio ψ may be defined by:

$$\psi = c\ (1-c)\ S_T\ \frac{\beta}{\alpha}. \tag{2}$$

The parameter ψ represents the ratio of the density gradient $\beta\ \nabla c_0$ produced by the concentration gradient and the density gradient $-\alpha\ \nabla T_0$ produced by the temperature gradient. Note that, in contrast to S_T, the sign of ψ is independent of whether the lighter or the heavier component is chosen as component 1 of the mixture, so that it is independent of which component is actually chosen to represent the concentration c of the mixture.

Finally, the Rayleigh number Ra is defined as:

$$Ra = -\frac{\alpha g L^4\ \nabla T_0}{\nu D_{\text{th}}}, \tag{3}$$

where L is the height of the liquid layer and g the gravitational acceleration constant. Note that the Rayleigh number is negative when $\nabla T_0 = dT_0/dz$ is positive, i.e., when the temperature gradient is pointing in the positive Z-direction, opposite to the direction of the gravitational force $\boldsymbol{g}$.

2.1 Linearized Random Boussinesq Equations for a binary liquid

We want to study small fluctuations around the thermally conducting state, i.e., fluctuations around the quiescent and stable state of the fluid. Following a notation adopted by some previous investigators [6,7,55], we denote the local fluctuation in the temperature T by $\theta\ (=\delta T)$, the local fluctuation in the z-component of the fluid velocity by $w\ (=\delta u_z)$ and the local fluctuation in the concentration c of component 1 of the mixture by $\Gamma\ (=\delta c)$. The fluctuations $\theta(\boldsymbol{r},t)$, $w(\boldsymbol{r},t)$ and $\Gamma(\boldsymbol{r},t)$ depend on the position $\boldsymbol{r}(x,y,z)$ and on the time t. In the spirit of Landau's fluctuating hydrodynamics [53], we may describe the space and time dependence of these fluctuations by the deterministic linearized random Boussinesq equations for a binary fluid supplemented with random noise terms [6–8,10]:

$$\begin{aligned}\frac{\partial}{\partial t}\left(\nabla^2 w\right) = \nu\ \nabla^2\left(\nabla^2 w\right) + g\ \left(\frac{\partial^2}{\partial x^2}+\frac{\partial^2}{\partial y^2}\right)\left[\alpha\,\theta - \beta\,\Gamma\right] + \\ + \frac{1}{\rho}\left\{\nabla\times\left[\nabla\times\left(\nabla\cdot\delta\mathsf{T}\right)\right]\right\}_z\,,\end{aligned} \tag{4a}$$

$$\frac{\partial \theta}{\partial t} = D_{\mathrm{th}}\ \nabla^2 \theta - w\ \nabla T_0 - \frac{D_{\mathrm{th}}}{\lambda_{\mathrm{T}}} \nabla(\delta \boldsymbol{Q}), \tag{4b}$$

$$\frac{\partial \Gamma}{\partial t} = D \left[\nabla^2 \Gamma + \frac{\alpha}{\beta} \psi\, \nabla^2 \theta \right] - w\ \nabla c_0 + \nabla(\delta \boldsymbol{J}), \tag{4c}$$

where λ_{T} is the thermal conductivity of the mixture. The notations ∇T_0 and ∇c_0 for the stationary gradients of temperature and concentration remind us that both ∇T_0 and ∇c_0 in (4) are constants and not gradients of locally fluctuating temperature and concentration. As in the standard fluctuating-hydrodynamics approach [53,54], we have included in (4) random noise terms to represent the contributions from rapidly varying short-range fluctuations [43,46,56–58]. Thus, we have introduced $\delta \mathsf{T}(\boldsymbol{r}, t)$ as the random stress tensor and $\delta \boldsymbol{Q}(\boldsymbol{r}, t)$ as the random heat flux following [56,57]. Additionally, we have introduced $\delta \boldsymbol{J}(\boldsymbol{r}, t)$ as the random solute flux following [43,46,58]. Note that the subscript z in (4a) indicates that the random noise term is to be identified with the z-component of the vector between curly brackets. This procedure of supplementing the random Boussinesq equations for a binary liquid with random noise terms was previously used by Schöpf and Zimmermann to study the influence of noise close to the convective instability [59]. We do not consider any pressure fluctuations in (4), since pressure fluctuations cause Brillouin scattering, but they do not contribute to the Rayleigh spectrum of the scattered light.

In applying the linearized random Boussinesq equations, as given by (4), we have assumed that all thermophysical properties of the binary fluid depend only weakly on temperature or concentration so that the variation of these properties as a function of z is negligible small; in practice this is a very good approximation [33]. For the same reason, in (2) the concentration c of component 1 represents an average value through the fluid layer; the substitution of the local concentration by an average concentration is only questionable for extremely dilute solutions [7]. Moreover, the Boussinesq approximation assumes the liquid to be incompressible [55], so the coefficient D_{th} in (4b) can indeed be identified with the thermal diffusivity $\lambda_{\mathrm{T}}/\rho c_{\mathrm{P}}$, where c_{P} is the specific isobaric heat capacity. As usual, the Dufour effect has been neglected in (4), since it is relevant only in binary gas mixtures and in liquids near the vapor-liquid critical point [11,60,61]. Following Chandrasekhar [55], to eliminate the hydrostatic pressure gradient we find it convenient to consider (4a) for $\nabla^2 w$, by taking a double curl in the equation for the fluctuating fluid velocity $\delta \boldsymbol{u}$.

2.2 Stability of the solution of the Linearized Boussinesq Equations

There is a considerable literature applying the linearized Boussinesq equations to binary systems, mainly focused on the analysis of the stability of the conductive solution (see, for instance, [6–11,62] and references therein). An excellent updated review, including nonlinear-stability analysis, has recently appeared in this Springer series of Lecture Notes in Physics [63]. The stability of the conductive solution depends on whether the temperature and concentration gradients are stabilizing or not. Thus, stability will depend on the sign of the Rayleigh

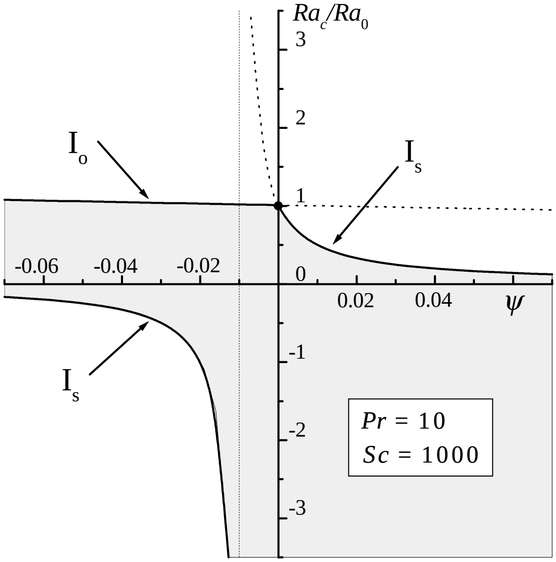

Fig. 1. Linear stability diagram deduced from the Boussinesq equations with free-slip-permeable boundary conditions for a binary liquid with typical values of the Schmidt and Prandtl numbers, according to [7]. The region of stability corresponds to the shadowed area.

number Ra and on the sign of the separation ratio ψ. In Fig. 1 we present the typical linear stability diagram in the $\{Ra, \psi\}$ plane, plotted after Schechter et al. [7]. The stability diagram depends on the values of the Schmidt and Prandtl numbers. The plot in Fig. 1 was obtained, as indicated, for Sc=1000 and Pr=10, which are typical values for an ordinary liquid mixture. Depending on the signs of Ra and ψ one can identify four regions in the diagram of Fig. 1:

1. If $Ra > 0$ and $\psi < 0$, the temperature gradient is destabilizing whereas the Soret-induced concentration gradient is weakly stabilizing. Note that if $\beta > 0$, S_T has to be negative to have an overall $\psi < 0$, see (2), and the denser component 1 migrates to the warm lower plate. If $\beta < 0$, the lighter component 1 migrates to the cold upper plate. In both cases the Soret effect is weakly stabilizing. In this situation, the instability appears at a nonzero horizontal wave number and at a nonzero frequency. The instability mechanism is thus an oscillatory periodic Hopf bifurcation or, in the language of Cross and Hohenberg [10], an $\mathrm{I_o}$-type instability. Above the threshold, the instability leads to a traveling-waves pattern [59].
2. When $Ra > 0$ and $\psi > 0$, both the temperature and the concentration gradient are destabilizing. For given ψ the instability appears at a lower Ra than in the case of a pure fluid ($\psi = 0$). In this situation the instability appears at a finite wave number but at zero frequency, as in a pure liquid: it is an $\mathrm{I_s}$-type instability. Above the threshold, the instability leads to a square pattern.

3. When $Ra < 0$ and $\psi < 0$, the temperature gradient is stabilizing, but the Soret coupling is destabilizing. For given Ra, the separation ratio ψ could be negative enough for an instability to appear. Note that this instability develops while heating the fluid from above, a configuration in which a pure liquid is always stable. As above, it is an $\mathrm{I_s}$-type instability. It was recently experimentally observed by La Porta and Surko [64].
4. Finally, when $Ra < 0$ and $\psi > 0$, both temperature and concentration gradients are stabilizing and the system is always in a quiescent stable state.
5. It is interesting to note the existence of a codimension-two instability point where the $\mathrm{I_o}$-instability line meets with the $\mathrm{I_s}$-instability line. In the linear approximation this happens on the $\psi = 0$ axis [65].

It is worth mentioning that the instability diagram depends on the boundary conditions. The diagram in Fig. 1 corresponds to free and permeable boundaries, which is mathematically the simplest case. For this particular case, the critical Rayleigh number Ra_c as a function of the separation ratio for the $\mathrm{I_o}$-instability line is given by [7]:

$$\left(\frac{Ra_\mathrm{c}}{Ra_0}\right)_\mathrm{o} = \frac{(1+Pr)(Sc+Pr)(1+Sc)}{Sc^2(\psi\; Pr + Pr + 1)}, \tag{5}$$

while the critical Rayleigh for the $\mathrm{I_s}$-instability line is given by [7]:

$$\left(\frac{Ra_\mathrm{c}}{Ra_0}\right)_\mathrm{s} = \frac{Pr}{Pr + \psi\;(Sc + Pr)} \tag{6}$$

with $Ra_0 = 27\pi^4/4$, the critical Rayleigh number for a pure fluid with free-slip boundary conditions [55]. These were the expressions employed to construct Fig. 1. The more realistic case of fixed and impermeable boundaries has also been analyzed [9,66]. But, as in the case of a pure fluid, different boundary conditions cause only quantitative differences while qualitatively the diagram is more or less the same. In addition, nonlinear terms that have been neglected in (4) cause also minor changes in the stability diagram, particularly shifting the position of the codimension-two instability point [65]. In any case, the preceding discussion of the relationship between stability and the signs of Ra and ψ still holds. The only situation for which stability is always assured is when $Ra < 0$ and $\psi > 0$. In this chapter we consider small fluctuations around the conductive state. Therefore, in the following, we shall assume $Ra < 0$ and $\psi > 0$, the situation in which fluctuations do not drive the system outside of a stable quiescent configuration.

2.3 Linearized Random Boussinesq Equations in the small-Lewis-number approximation

In principle, it is possible to calculate the structure factor of the binary liquid from the system of coupled differential equations given by (4), as was done in the simpler case of a pure liquid [41]. However, there are several complications which make the calculation here more involved. A first complication arises from the fact that, since they have the same tensorial character, the random heat flux $\delta \boldsymbol{Q}$ and the random solute flux $\delta \boldsymbol{J}$ are coupled and their cross-correlations are not zero: $\langle \delta Q_i \cdot \delta J_j \rangle \neq 0$ [43,58]. (But note that under some approximations these cross correlations may be neglected, as done by Schöpf and Zimmermann [59]). A second complication is that density or refractive-index fluctuations come from both temperature *and* concentration fluctuations; hence, these two types of fluctuations have to be calculated, contrary to the case of a pure liquid, where there are no concentration fluctuations. As mentioned in the introduction, in the case of binary liquid systems, the diffusion coefficient D is much smaller than the thermal diffusivity D_{th} and the kinematic viscosity ν. Hence, to obtain the structure factor of a binary liquid system we can consider to a very good approximation the limit of vanishing Lewis number $Le = D/D_{\mathrm{th}}$. Since $\nu > D_{\mathrm{th}}$, a small value of the Lewis number Le also implies a small value of the inverse Schmidt number $Sc^{-1} = D/\nu$.

Velarde and Schechter [52] have considered the Boussinesq equations of a liquid mixture for small values of the Lewis number. By supplementing the hydrodynamic equations obtained in [52] with the corresponding random noise terms, one deduces from (4) in the limit $Le \to 0$:

$$0 = \nu \, \nabla^2 \left(\nabla^2 w \right) - \beta g \left(\frac{\partial^2 \Gamma}{\partial x^2} + \frac{\partial^2 \Gamma}{\partial y^2} \right) + \frac{1}{\rho} \left\{ \nabla \times \left[\nabla \times \left(\nabla \cdot \delta \mathsf{T} \right) \right] \right\}_z , \tag{7a}$$

$$\frac{\partial \Gamma}{\partial t} = D \, \nabla^2 \Gamma - w \, \nabla c_0 + \nabla \delta \boldsymbol{J}. \tag{7b}$$

In the limit $Le \to 0$, any coupling between the concentration fluctuations and the temperature fluctuations vanishes and one only needs to consider coupling between the concentration fluctuations and the transverse-velocity fluctuations, as mentioned in the introduction. Moreover, since the transverse-velocity fluctuations decay much faster than the concentration fluctuations, one does not need to include the viscous mode directly in the dynamic structure factor, but only its indirect effect on the concentration fluctuations. That is, in the limit $Sc^{-1} \to 0$ the time derivative $\partial/\partial t (\nabla^2 w)$ on the left-hand side of (7a) can be neglected.

We may mention that the small-Lewis-number approximation has been amply used in the literature to simplify the study of the stability of binary liquid mixtures [7,52,65,67]. As discussed in the literature [7,52], the $Le \to 0$ approximation has several shortcomings; in particular, it does not describe correctly the situation with $Ra > 0$ and $\psi < 0$, missing the interesting Hopf bifurcation and codimension-two instability point. But in this chapter we are only concerned with the case $Ra < 0$ and $\psi > 0$, that is, the case of the quiescent stable thermally conducting state, for wich the $Le \to 0$ approximation is adequate to describe the concentration fluctuations, as will be demonstrated in the subsequent sections.

2.4 Calculation of the structure factor

Having introduced the hydrodynamic simplifications described in Sect. 2.3, we can now readily calculate the structure factor of the binary liquid, following a procedure similar to the one adopted in a previous publication [41] in the case of a one-component liquid. In the absence of any boundary conditions we apply a temporal and spatial Fourier transformation to (7) so as to obtain:

$$\begin{pmatrix} -\nu\ q^4 & -\beta\ g\ q_\parallel^2 \\ \nabla c_0 & i\omega + D\ q^2 \end{pmatrix} \begin{pmatrix} w(\omega,\boldsymbol{q}) \\ \Gamma(\omega,\boldsymbol{q}) \end{pmatrix} = \begin{pmatrix} F_1(\omega,\boldsymbol{q}) \\ F_2(\omega,\boldsymbol{q}) \end{pmatrix}, \tag{8}$$

with $q_\parallel$ representing the magnitude of the wave vector $\boldsymbol{q}$ in the XY plane, i.e., $q_\parallel^2 = q_x^2 + q_y^2$. To simplify the notation, we have introduced in (8) Langevin random noise terms F_1 and F_2, which are related to the Fourier transforms of the random stress tensor $\delta\mathsf{T}(\omega,\boldsymbol{q})$ and of the random solute flux $\delta\boldsymbol{J}(\omega,\boldsymbol{q})$ by:

$$\begin{pmatrix} F_1(\omega,\boldsymbol{q}) \\ F_2(\omega,\boldsymbol{q}) \end{pmatrix} = \begin{pmatrix} i\ \rho^{-1}\ \left\{q_z\, \boldsymbol{q}\cdot[\boldsymbol{q}\cdot\delta\mathsf{T}(\omega,\boldsymbol{q})] - q^2\,[\boldsymbol{q}\cdot\delta\mathsf{T}(\omega,\boldsymbol{q})]_z\right\} \\ -i\ \boldsymbol{q}\cdot\delta\boldsymbol{J}(\omega,\boldsymbol{q}) \end{pmatrix}. \tag{9}$$

Since we have adopted the small-Lewis-number approximation, the temperature fluctuations can be neglected and the Rayleigh component $S(\omega,\boldsymbol{q})$ of the structure factor can be attributed to refractive-index fluctuations caused by the concentration fluctuations only. Hence, the relationship between $S(\omega,\boldsymbol{q})$ and the autocorrelation function $\langle\Gamma^*(\omega,\boldsymbol{q})\cdot\Gamma(\omega',\boldsymbol{q}')\rangle$ of the concentration fluctuations is simply given by:

$$\langle\Gamma^*(\omega,\boldsymbol{q})\cdot\Gamma(\omega',\boldsymbol{q}')\rangle = \left(\frac{\partial c}{\partial n}\right)_T^2\ S(\omega,\boldsymbol{q})\ (2\pi)^4\ \delta(\omega-\omega')\ \delta(\boldsymbol{q}-\boldsymbol{q}'). \tag{10}$$

To deduce the autocorrelation $\langle\Gamma^*(\omega,\boldsymbol{q})\cdot\Gamma(\omega',\boldsymbol{q}')\rangle$ of the concentration fluctuations from (8), we need the correlation functions for the Langevin noise terms F_1 and F_2. They can be calculated from the known correlation functions between the different components of the random stress and the random solute flux. In nonequilibrium fluctuating hydrodynamics it is assumed that the correlation functions of the random stress tensor and the random solute flux retain their local equilibrium values [43]. From the expressions for the correlation functions of the random stress tensor $\delta\mathsf{T}$ as, for instance, given by (3.12) in [56] and for the correlation functions of the random solute flux $\delta\boldsymbol{J}$, as given by [43,58], and using the definition (9) of the Langevin noise terms, we obtain:

$$\begin{aligned}
\langle F_1^*(\omega,\boldsymbol{q})\cdot F_1(\omega',\boldsymbol{q}')\rangle &= 2k_\mathrm{B}T\frac{\nu}{\rho}\ q_\parallel^2\ q^4\ (2\pi)^4\ \delta(\omega-\omega')\ \delta(\boldsymbol{q}-\boldsymbol{q}'),\\
\langle F_2^*(\omega,\boldsymbol{q})\cdot F_2(\omega',\boldsymbol{q}')\rangle &= 2k_\mathrm{B}T\frac{D}{\rho}\left(\frac{\partial c}{\partial \mu}\right)_T\ q^2\ (2\pi)^4\ \delta(\omega-\omega')\ \delta(\boldsymbol{q}-\boldsymbol{q}'),\\
\langle F_1^*(\omega,\boldsymbol{q})\cdot F_2(\omega',\boldsymbol{q}')\rangle &= \langle F_2^*(\omega,\boldsymbol{q})\cdot F_1(\omega',\boldsymbol{q}')\rangle = 0,
\end{aligned} \tag{11}$$

where $\mu = \mu_1 - \mu_2$ is the difference between the chemical potential μ_1 per unit mass of component 1 and the chemical potential μ_2 per unit mass of component

2, while k_B is Boltzmann's constant. Note that the correlations between the random noise terms F_1 and F_2 are short ranged both in space and in time so that they can be represented by delta functions. Now, inverting (8) and using (10) and (11) one obtains for the dynamic structure factor $S(\omega, \boldsymbol{q})$ for the Rayleigh scattering in the binary liquid:

$$S(\omega, \boldsymbol{q}) = \left(\frac{\partial n}{\partial c}\right)_T^2 \frac{2k_\mathrm{B}T}{\rho} \frac{Dq^2 \left[\left(\frac{\partial c}{\partial \mu}\right)_T + \frac{(\nabla c_0)^2\, q_\parallel^2}{\nu D\, q^6}\right]}{\omega^2 + D^2 q^4 \left(1 - \psi \frac{Ra}{Le} \frac{\tilde{q}_\parallel^2}{\tilde{q}^6}\right)^2}. \tag{12}$$

In the denominator of (12) we have introduced a dimensionless wave number $\tilde{q} = qL$, so as to express the effect of gravity g through the Rayleigh number defined by (3), thus facilitating a comparison with previous work [46,49]. The quantity $\psi Ra/Le$ in (12) is given by:

$$\psi \frac{Ra}{Le} = -\psi \frac{D_\mathrm{th}}{D} \frac{\alpha g L^4\ \nabla T_0}{\nu\ D_\mathrm{th}} = \frac{\beta g L^4\ \nabla c_0}{\nu\ D}. \tag{13}$$

A convective instability will appear when the expression (12) for $S(\omega, \boldsymbol{q})$ diverges for some finite value of q. For such a divergence to appear it is required that $\beta\ \nabla c_0 > 0$, i.e., the concentration of the heavier component has to be higher above. This is the so-called salt-fountain, double-diffusive, or salt-fingers instability [7,62,65]. In our case it appears driven by the Soret effect, but it can also be studied in a more general context considering a concentration gradient independent of the temperature gradient, in which case it is called the thermohaline problem [7,68]. However, we are here considering the situation with $Ra < 0$ (thus $\alpha\ \nabla T_0 > 0$) and $\psi > 0$, so that in our case analyticity of (12) is always assured.

Note that, although we have assumed that the stationary concentration gradient appears through the Soret effect, upon substitution of (13) in (12), our final result for the dynamic structure factor $S(\omega, \boldsymbol{q})$ can be written in a form in which ∇T_0 and ψ do not appear explicitly. This fact suggests that our result will be valid whenever there exists a concentration gradient in the system, independent of whether it is induced by the Soret effect or by any other cause. Hence, we may compare our present results with those of Vailati and Giglio [49], who considered nonequilibrium concentration fluctuations in an isothermal free-diffusion process. We find agreement between our present result (12), and equation (24) of Vailati and Giglio [49] for the contribution of the nonequilibrium concentration fluctuations to the Rayleigh spectrum of scattered light. Vailati and Giglio also obtained a second Lorentzian contribution due to the viscous fluctuation. We have neglected this contribution here, since the hydrodynamic approximation employed by us means in practice a small value of the inverse Schmidt number $Sc^{-1} = D/\nu$. If we would have retained $\partial/\partial t(\nabla^2 w)$ on the left-hand side of (7a) we would have recovered this second Lorentzian contribution as well. A minor difference with the result of Vailati and Giglio is that the latter have assumed small scattering angles, so that $q_{\|} \simeq q$. Equation (12) for $S(\omega, \boldsymbol{q})$ is the generalization to arbitrary scattering angles. The fact that our result for the nonequilibrium Rayleigh spectrum in a binary liquid in the presence of a temperature gradient appears to be identical to that for the isothermal case with a concentration gradient is a direct consequence of the $Le \to 0$ approximation, which neglects the temperature fluctuations and its coupling with concentration fluctuations.

By integrating (12) over all frequencies ω, we obtain for the static structure factor of a nonequilibrium binary liquid due to concentration fluctuations:

$$S(\boldsymbol{q}) = S_{\mathrm{E}} \left\{ 1 + \tilde{S}_{NE}(\boldsymbol{q}) \right\}, \tag{14}$$

with

$$\tilde{S}_{\mathrm{NE}}(\boldsymbol{q}) = \left[\left(\frac{\partial \mu}{\partial c} \right)_T \frac{(\nabla c_0)^2}{\nu\ D} - \frac{\beta\ g\ \nabla c_0}{\nu\ D} \right] \frac{1}{1 - \psi \dfrac{Ra}{Le} \dfrac{\tilde{q}_{\|}^2}{\tilde{q}^6}} \frac{q_{\|}^2}{q^6}. \tag{15}$$

In (14) and (15), S_{E} is the equilibrium structure factor which is obtained when $\nabla c_0 = 0$, and $\tilde{S}_{\mathrm{NE}}$ represents the normalized nonequilibrium contribution to the structure factor, which is a dimensionless quantity referred to as nonequilibrium enhancement in several publications [34,51]. As in the case of the dynamic structure factor (12), our result (15) for the static structure factor will be valid only in the $\{Ra < 0, \psi > 0\}$ quadrant of the stability diagram in Fig. 1. In any other case a Soret-driven double diffusive instability will appear as a divergence in the structure factor for some finite value of $q_{\|}$. A problem is that (15) has also no divergence for $Ra > 0$ and $\psi < 0$, where a instability in the form of a Hopf bifurcation is expected [7,10,63,65]. The fact that we do not find this instability here is a consequence of the $Le \to 0$ approximation [7,52]. Also in deriving (15) we did not take into account finite-size effects. Linear instability theory of the binary Boussinesq equations suggests that, when boundary conditions are considered together with (7), a modified structure factor could be calculated which would be valid in some bounded region outside the $\{Ra < 0, \psi > 0\}$ quadrant (the region where the conductive solution is stable). Again as before, the static structure factor given by (15) can be written in such a way that it depends explicitly only on the value of the stationary concentration gradient ∇c_0 and not on ψ or ∇T_0. Consequently (15) can be also employed to analyze nonequilibrium concentration fluctuations in isothermal diffusion processes [69–71].

As will be shown in Section 3, for the interpretation of several light-scattering experiments in liquids far away from any convective instability we may neglect the effects of gravity by taking the limit $g \to 0$. In this limit (15) reduces to:

$$\tilde{S}_{\mathrm{NE}}(\boldsymbol{q}) = \left(\frac{\partial \mu}{\partial c} \right)_T \frac{(\nabla c_0)^2}{\nu\ D} \frac{q_{\|}^2}{q^6}, \tag{16}$$

which has been verified experimentally [51], as further discussed below. Note that (16), contrary to (15), does not include any divergence and is valid for any positive or negative value of ∇c_0. This is expected since in the derivation of (16) gravity was neglected, so that the system is always in a stable quiescent state.

We remark that the derivation of the structure factor from (7) described above can just as easily be implemented without neglecting the time derivative $\partial/\partial t(\nabla^2 w)$ on the left-hand side of (7a). Instead of (16) we would then have obtained:

$$\tilde{S}_{\mathrm{NE}}(\boldsymbol{q}) = \left(\frac{\partial \mu}{\partial c}\right)_T \frac{(\nabla c_0)^2}{(\nu^2 - D^2)} \frac{\nu}{D} \frac{q_\parallel^2}{q^6}, \tag{17}$$

which for $\nu \gg D$ reduces to (16). We have preferred to perform the derivation in the way it was done to retain consistency with the hydrodynamic approximations as originally introduced by Velarde and Schechter [52].

As already pointed out, the various expressions derived here for the contribution of the nonequilibrium concentration fluctuations to the structure factor are valid for wave numbers q such that $qL \ll 1$. When qL becomes of order unity, finite-size effects need to be considered which depend to some extent on the nature of the boundary conditions [41,42]. Finite-size effects on the nonequilibrium concentration fluctuations in binary liquids will be considered in a future publication [47].

3 Experiments

During the past years several experimental results on nonequilibrium Soret-driven concentration fluctuations have appeared in the literature. The goal of this section is to make a comparison between experimental results and the theory developed in Sect. 2. Two different experimental techniques have been employed to study nonequilibrium concentration fluctuations in liquid mixtures: light scattering and, more recently, quantitative shadowgraph analysis. Experiments have been performed with binary liquid mixtures and with dilute polymer solutions. In the case of dilute polymer solutions, as long as the concentration is low enough to neglect entanglements, an hydrodynamic approach of the type described in Sect. 2 should be applicable.

3.1 Experimental techniques

A nonequilibrium enhancement of the concentration fluctuations in binary liquid systems has indeed been observed by small-angle light-scattering experiments [34,35,39,40,50,51]. A schematic representation of such a light-scattering experiment is shown in Fig. 2. The scattering medium is a thin horizontal fluid layer bounded by two parallel plates of high thermal conductivity. The temperatures of the plates T_1 and T_2 can be controlled independently so as to establish a temperature gradient across the fluid layer in the vertical direction, parallel or antiparallel to the direction of gravity. The horizontal plates are furnished with windows allowing a laser beam to propagate through the fluid in the direction

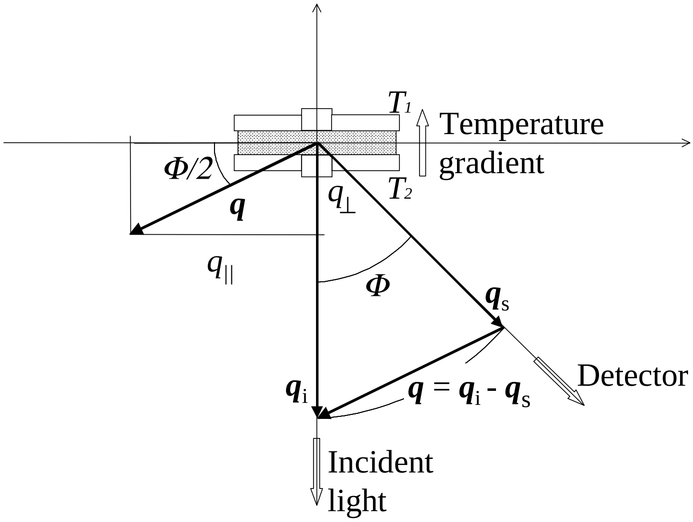

Fig. 2. Schematic representation of a low-angle nonequilibrium light-scattering experiment. $\boldsymbol{q}_{\rm i}$ is the wave vector of the incident light, $\boldsymbol{q}_{\rm s}$ is the wave vector of the scattered light. The magnitude $q = |\boldsymbol{q}_{\rm i} - \boldsymbol{q}_{\rm s}|$ of the scattering wave vector is related to the scattering angle Φ by $q = 2q_0 \sin(\Phi/2)$, where q_0 is the magnitude of the wave vector $\boldsymbol{q}_{\rm i}$ of the incident light inside the liuqid. For clarity, the scattering angle Φ has been exaggerated.

(anti)parallel to the temperature gradient. Light scattered over an angle Φ arises from fluctuations with a wave number q such that [72]:

$$q = 2q_0 \sin(\Phi/2), \tag{18}$$

where q_0 is the wave number of the incident light inside the fluid medium. Due to the dependence of the nonequilibrium enhancement (16) of the structure factor on q^{-4}, to observe any nonequilibrium enhancement one needs to measure the scattered light at small wave numbers and, hence, at very small scattering angles Φ. In practice this means that one measures the structure factor at $q_{||} = q$ and $q_\perp = 0$, where $q_\perp$ is the component of the wave vector $\boldsymbol{q}$ along the vertical direction. The need for very small scattering angles complicates the experimental technique. To avoid uncertainties in the scattering angle due to laser beam bending inside the sample the two horizontal plates need to be parallel to a high degree and the laser beam has to be carefully aligned perpendicularly to the windows. In addition, at these small scattering angles stray scattering from window surfaces is dominant. Thus to obtain enough signal to background ratio great care is required to have always very clean windows.

Nonequilibrium concentration fluctuations can be observed by both static and dynamic light scattering. For static light scattering a photodiode array can be employed to measure the total intensity of light. For dynamic light scattering the light collected in the detector has to be analyzed with a correlator. In the experiments one first measures the equilibrium light scattering by maintaining the temperatures of the two horizontal plates at the same value, $T_1 = T_2$. Subsequently, a temperature gradient is established by independently changing the temperatures of the two plates bounding the fluid layer. Comparing the intensity of light collected in the detector (or the amplitude of the autocorrelation function of the scattered light in dynamic experiments) in thermal equilibrium and out of thermal equilibrium, experimental values for the nonequilibrium enhancement are obtained.

Recently nonequilibrium concentration fluctuations have also been investigated by a shadowgraph projection technique [70]. The experimental arrangement is similar to the one depicted in Fig. 2, but instead of a laser beam, an extended uniform monochromatic light source is employed to illuminate the sample. Then many shadowgraph images of a plane perpendicular to the temperature gradient are obtained with a charge coupled device (CCD) detector, which measures a spatial distribution of intensity $I(\boldsymbol{x})$, where here $\boldsymbol{x}$ is a two-dimensional position vector in the imaging plane. For each image a shadowgraph signal is defined by:

$$i(\boldsymbol{x}) = \frac{I(\boldsymbol{x}) - I_0(\boldsymbol{x})}{I_0(\boldsymbol{x})}, \tag{19}$$

where $I_0(\boldsymbol{x})$ is the blank intensity distribution, when there are no fluctuations in the index of refraction of the sample. In practice $I_0(\boldsymbol{x})$ is obtained by averaging over many shadowgraph images, so that fluctuations cancel out and the resulting $I_0(\boldsymbol{x})$ contains only contributions coming from nonuniform illumination of the sample. Using physical and geometrical optics one can demonstrate that the modulus squared of the two-dimensional Fourier transform of the shadowgraph signal, $|i(\boldsymbol{q})|^2$, taking an azimuthal average can be expressed as [70,73,74]:

$$\overline{|i(\boldsymbol{q})|^2} = \hat{T}(q)\ S(q_{\|} = q, q_{\perp} = 0). \tag{20}$$

The azimuthal average of $|i(\boldsymbol{q})|^2$, indicated by the overline, depends only on the modulus q of the two-dimensional Fourier vector $\boldsymbol{q}$. The symbol $\hat{T}(q)$ represents an optical transfer function, which can be derived from the optical arrangement employed to produce the shadowgraph pictures; it includes contributions from the response of the CCD detector and from the dependence of the refractive index on temperature and concentration [70,74]. Therefore, from an analysis of the spectrum of the shadowgraph pictures one can determine the structure factor of the fluid in the plane $q_{\perp} = 0$.

We note that quantitative shadowgraph experiments so far performed by Brogioli et al. [70] refer to nonequilibrium concentration fluctuations not induced by the Soret effect, but induced by free diffusion. Nevertheless, as mentioned in Sect. 2.4, the final theoretical result, given by (15), depends only on the value of the stationary concentration gradient ∇c_0. Hence, this equation remains valid independently of whether the concentration gradient is induced by a temperature gradient through the Soret effect or by any other process, as in a free-diffusion process. Equation (15) has indeed been employed successfully to analyze nonequilibrium concentration fluctuations in diffusion processes [69]. For these reasons, and also because this newly developed experimental technique is perfectly suited for the study of nonequilibrium concentration fluctuations induced by thermodiffusion we have briefly sketched the fundamentals of the shadowgraph method.

There is an equivalence between small-angle light-scattering and shadowgraph experiments, in the sense that both methods give us $S(q_{\|} = q, q_{\perp} = 0)$, where for light scattering q is the scattering wave vector as given by (18), whereas for shadowgraph techniques q is the modulus of the two-dimensional Fourier vector in the imaging plane. As mentioned by Bodenschatz et al., what it is measured in the experiments is a kind of vertical average of the fluctuations [61].

3.2 Nonequilibrium concentration fluctuations in binary liquid mixtures

Experimental measurements of the nonequilibrium enhancement of the concentration fluctuations induced by the Soret effect in binary liquid mixtures have been independently obtained at the University of Maryland [34,35,75,76] and at the University of Milan [39,40]. At the University of Maryland, Sengers and coworkers have performed nonequilibrium Rayleigh-scattering experiments in mixtures of liquid toluene and liquid n-hexane, far from the critical point of demixing. Because they used dynamic techniques, they were able to determine not only the enhancement of the scattering due to the nonequilibrium concentration fluctuations, but also the contribution from the nonequilibrium viscous and temperature fluctuations. In this mixture the Lewis number is about $Le = 3 \times 10^{-2}$ which is small enough for the viscous and temperature fluctuations to decay sufficiently fast so as to enable an independent determination of the nonequilibrium enhancement of the concentration fluctuations directly from the long-time behavior of the autocorrelation function of the scattered-light intensity. A compilation of the experimental values obtained for the magnitude of the nonequilibrium enhancement of the concentration fluctuations , designated by A_c and to be identified with $\tilde{S}_{\mathrm{NE}}$ as given by (16) or (17), can be found in Tables IV-VI of [35] for various values of the temperature gradient ∇T_0, the wave number q and the average concentration c. In these experiments the wave number q was large enough so that gravity effects could be neglected, but at the same time sufficiently small to identify q with $q_{\|}$ and neglect $q_{\perp}$. It thus follows from (16) or (17) that $\tilde{S}_{\mathrm{NE}} = A_c$ should be proportional to $(\nabla T_0)^2/q^4$:

$$\tilde{S}_{\mathrm{NE}} \propto \frac{\nabla T_0^2}{q^4}. \tag{21}$$

As an illustration, we show in Fig. 3 observed values of $\tilde{S}_{\mathrm{NE}} = A_c$ as a function of $(\nabla T_0)^2/q^4$ obtained for two concentrations of the mixture toluene + n-hexane at 25°C [35]. The experiments confirm that the nonequilibrium enhancement of the concentration fluctuations is indeed directly proportional to $(\nabla T_0)^2$ and inversely proportional to q^4 [34,35,75,76]. Note that the q^{-4} dependence for small q, verified by Fig. 3, means that the correlations in real space are long-ranged, encompassing the entire system not involving any intrinsic length

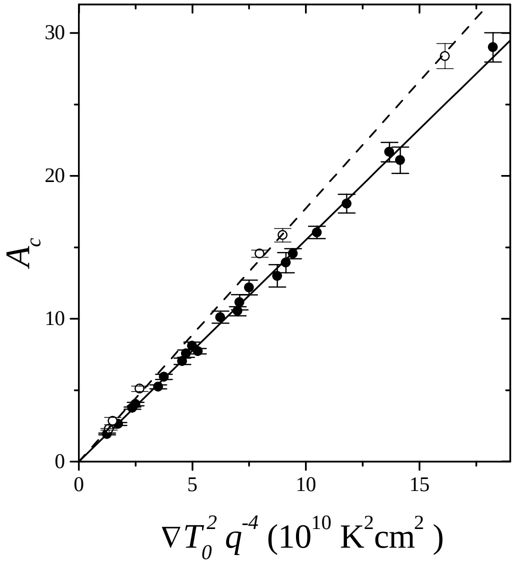

Fig. 3. Nonequilibrium enhancement of the concentration fluctuations A_c as a function of $\nabla T_0^2 q^{-4}$ at two different concentrations of toluene in n-hexane. The open symbols are for a mole fraction of toluene $x = 0.5$ and the filled symbols are for a mole fraction of toluene $x = 0.75$. The solid lines represent linear fits to the data. From [35].

scale, only quenched by finite-size effects when q becomes of the order L^{-1}, the finite height of the system acting as a natural cutoff for the wave vector of the fluctuations [41,42,47].

For a quantitative interpretation of the observed nonequilibrium enhancement of the concentration fluctuations one needs reliable values for the derivative $(\partial\mu/\partial c)_T$, the kinematic viscosity ν, the mass diffusion coefficient D and the Soret coefficient S_T. An accurate optical beam-bending method was developed to measure D and the Soret coefficient S_T of the liquid mixture [77], but data for $(\partial c/\partial\mu)_T$ and ν had to be deduced from the literature [35]. In spite of these efforts a quantitative confirmation of the accuracy of the prefactors in (16) and (17) has not yet been obtained for liquid mixtures [34,35,75,76], but it has been obtained for polymer solutions, as will be further discussed below [50,51].

Vailati and Giglio measured nonequilibrium concentration fluctuations induced by the Soret effect in a mixture of liquid aniline and cyclohexane [39,40]. Light-scattering experiments were performed in the homogeneous phase, but not very far from the critical consolute point. Due to critical slowing down, concentration fluctuations are dominant in this situation, assuring no contribution of temperature or viscous fluctuations to the total scattering intensity. This scenario corresponds to a negligibly small Lewis number and the light-scattering intensity should be given by (15). In addition, the experimental device used by Vailati and Giglio allowed them to measure the scattering intensity at angles sufficiently small to observe gravity effects. To simplify the analysis of the experiments, Vailati and Giglio introduced a "roll-off" scattering wave number defined as [39]:

$$q_{\mathrm{RO}}^4 = -\frac{\beta\, g\, \nabla c_0}{\nu\, D} = -\psi \frac{Ra}{Le} \frac{1}{L^4}. \tag{22}$$

Note again that the experiments are performed for $Ra < 0$ and $\psi > 0$, so that the right-hand side of (22) is positive and q_{RO} is a real quantity. With this definition, we obtain from (15):

$$\tilde{S}_{\mathrm{NE}} \propto \frac{\nabla T_0^2}{q^4 + q_{\mathrm{RO}}^4}. \tag{23}$$

Note that for large q (23) reduces to (21). But, in the limit $q \to 0$, the q^{-4} divergence in (21) becomes saturated and (23) predicts that a constant limiting value for $\tilde{S}_{\mathrm{NE}}$ will be reached [46].

The difference between the equilibrium and the nonequilibrium intensity of the scattered light, which is proportional to $\tilde{S}_{\mathrm{NE}}$ as measured by Vailati and Giglio [39] for a mixture of aniline and cyclohexane is shown in Fig. 4 as a function of the wave number q. The solid curve represents a fit to (23). Because of the small scattering angles covered in this experiment, the crossover from a q^{-4} divergence to the gravitationally induced saturation at very small q is clearly observed. From the fit of (23) to the experimental data, Vailati and Giglio deduced $q_{\mathrm{RO}} = 537\ \mathrm{cm}^{-1}$, which is close to the theoretical value $q_{\mathrm{RO}} = 410\ \mathrm{cm}^{-1}$

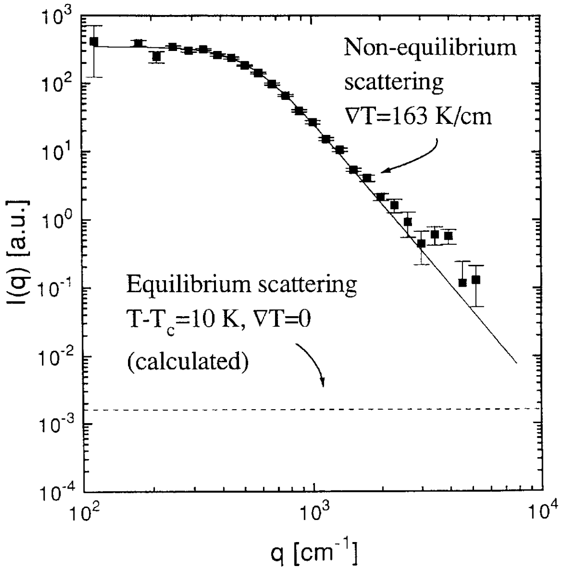

Fig. 4. Difference between nonequilibrium and equilibrium intensity of scattered light for a mixture of aniline and cyclohexane as a function of the scattering vector. The symbols represent experimental data obtained with $\nabla T_0 = 163\ \mathrm{K\ cm}^{-1}$. the solid curve represents a fit to (23). Reproduced with permission from [39].

they obtained from (22) using literature values for the thermophysical properties of this mixture. We should note that $\tilde{S}_{\mathrm{NE}}$ is plotted in Fig. 4 in arbitrary units. The authors did not have the resolution to determine the absolute magnitude of the nonequilibrium enhancement of the concentration fluctuations with sufficient accuracy to make a reliable check of the validity of the prefactor in (16) or (17).

3.3 Nonequilibrium concentration fluctuations in dilute polymer solutions

Experimental values for the nonequilibrium enhancement $\tilde{S}_{\mathrm{NE}}$ of concentration fluctuations have been obtained for dilute solutions of polystyrene ($M_W =$ 96 400) in toluene from low-angle dynamic light-scattering at the University of Maryland [51,50,78]. As described in Sect. 3.1, the nonequilibrium enhancements were determined by comparing the observed amplitude of the time correlation function measured in equilibrium and out of equilibrium. The experimental values thus obtained for $\tilde{S}_{\mathrm{NE}}$ at 25°C can be found in Table II of [50], where they are denoted again by A_c.

To make a quantitative comparison of the experimental data with the theoretical expression (16) for $\tilde{S}_{\mathrm{NE}}$, we have presented in Table 1 values for the various thermophysical properties of the polymer solutions at various polymer concentrations collected from the literature [50,79,80]. In this Table S_T represents the Soret coefficient of the polymer in toluene as the solvent, as measured by Zhang et al. [80] by an optical beam-bending technique. The values for the solute expansion coefficient β in Table 1 were calculated from an empirical correlation for the dependence of the density ρ on the concentration, at 25°C, proposed by Scholte [79]. For the other properties, we refer to [50]. If we estimate the thermal expansion coefficient α of the polymer solution by the value corresponding to pure toluene at 25°C: $\alpha = 0.97 \times 10^{-3}$ K^{-1}, we note from (2) that the separation ratio ψ is positive, ranging from $\psi = 0.121$ for $c = 0.25\%$ to $\psi = 1.101$ for $c = 4.00\%$. Hence, the polymer solution is indeed in a stable thermally conducting state when heated from above (i.e., $Ra < 0$). If we estimate the thermal diffusivity of the dilute solution by the value $D_{\mathrm{th}} = 0.89 \times 10^{-3}$ cm^2

Table 1. Thermophysical properties of a solution of polystyrene ($M_W =$ 96 400) in toluene at 25°C at several polymer concentrations c, as obtained from various literature sources [50].

c (w/w)	$(\frac{\partial\mu}{\partial c})_T$ cm^2 s^{-2}	D cm^2 s^{-1}	ν cm^2 s^{-1}	S_T K^{-1}	ρ^{a} g cm^{-3}	β (w/w)$^{-1}$
0.005	7.48×10^7	5.16×10^{-7}	7.71×10^{-3}	0.218	0.8627	−0.208
0.015	4.41×10^7	6.01×10^{-7}	10.8×10^{-3}	0.178	0.8645	−0.209
0.020	4.16×10^7	6.51×10^{-7}	12.6×10^{-3}	0.167	0.8654	−0.209
0.040	4.25×10^7	8.32×10^{-7}	21.4×10^{-3}	0.132	0.8690	−0.209

[a] From Scholte [79].

s^{-1} corresponding to pure toluene at 25°C, we conclude that $Le \simeq 7 \times 10^{-4}$. Hence the assumption of small Lewis number is well justified and (16) agrees indeed with the experimental data [50,51,78].

An elegant comparison between theory and experiment can be obtained in terms of a scaled universal representation of $\tilde{S}_{\mathrm{NE}}$ adopted by Brogioli et al. [70] for studying concentration fluctuations in free-diffusion processes. For this purpose we note that (15), with the definition (22) for q_{RO} and the small-angle approximation $q_{\|} \simeq q$, can be rewritten as:

$$\frac{\tilde{S}_{\mathrm{NE}}(s)}{\tilde{S}_{\mathrm{NE}}^{0}} = \frac{1}{1+s^4} \tag{24}$$

with

$$\tilde{S}_{\mathrm{NE}}^{0} = 1 + \left(\frac{\partial \mu}{\partial c}\right)_T \frac{\left(\nabla c_0\right)^2}{\nu D\, q_{\mathrm{RO}}^4}, \tag{25}$$

where $s = q/q_{\mathrm{RO}}$ is a scaled wave number. We note that $\tilde{S}_{\mathrm{NE}}^{0}$ given by (25) simply represents the nonequilibrium enhancement of the concentration fluctuations in the limit $q \to 0$.

The scale factors $\tilde{S}_{\mathrm{NE}}^{0}$ and q_{RO} in (24) depend on the thermophysical properties of the solution and on the value of the stationary concentration gradient ∇c_0, which in turn depends on the applied stationary temperature gradient ∇T_0 through the Soret coefficient S_T in accordance with (1). For each pair of values c and ∇T_0, q_{RO} and $\tilde{S}_{\mathrm{NE}}^{0}$ can be calculated from the literature data presented in Table 1. If we then scale the experimental data for $\tilde{S}_{\mathrm{NE}}$ by $\tilde{S}_{\mathrm{NE}}^{0}$ and the wave number q by q_{RO}, a universal curve should be obtained according to (24). We have performed such an analysis for the experimental data obtained for the polystyrene solution in toluene [50] and the results are shown in Fig. 5. The insert in Fig. 5 shows in more detail the data in the actual range of experimental wave numbers. To make Fig. 5 more legible we have plotted only experimental data corresponding to three polymer concentrations, but there is no difference if the data obtained for all different polymer solutions are included. It should be emphasized that the curve in Fig. 5, unlike the ones in Fig. 3 or in Fig. 4, is not a fit of the experimental data but is just the universal function defined in (24). Although the experiment does not cover small enough wave numbers for the saturation effect due to gravity to be observed, Fig. 5 does show excellent agreement between theory and experiment. In fact, the light-scattering data obtained for the polystyrene solution in toluene represent the first accurate confirmation of the theory for the nonequilibrium concentration fluctuations, including the prefactor in (16).

3.4 Observation of nonequilibrium concentration fluctuations by shadowgraphy

Before closing we wish to comment shortly on the recent observation of nonequilibrium concentration fluctuations by Brogioli et al. from a quantitative shad-

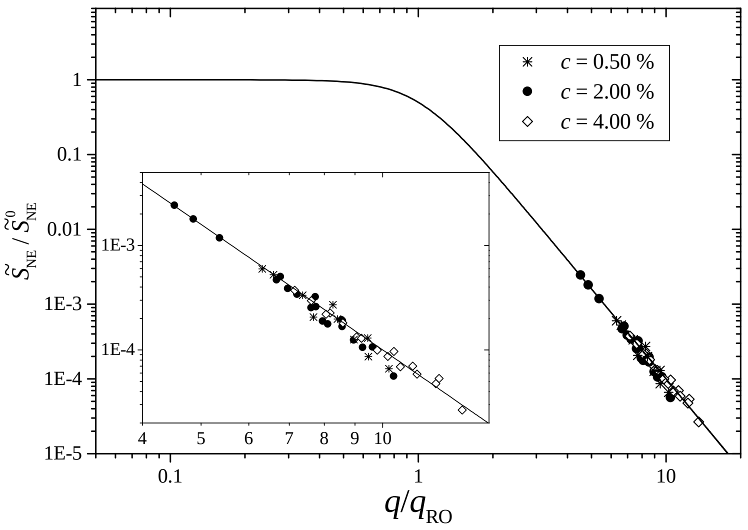

Fig. 5. Value of the scaled nonequilibrium enhancement of the concentration fluctuations as a function of the scaled scattering wave number for solutions of polystyrene in toluene at several concentrations. The solid curve represents the universal function (24). The insert shows the range were the actual experimental data have been obtained [50].

owgraph analysis [70]. As earlier mentioned, this work is concerned with concentration gradients induced not by the Soret effect, but by a free-diffusion process. The experimental setup is similar to the one depicted in Fig. 2 with the exception that both plates are maintained at the same temperature. Brogioli et al. studied free-diffusion in pure water of concentrated aqueous solutions of several solutes, including glycerol and the polymer PolyEthyleneGlycol. The initial state was prepared by filling the cell with the lighter liquid and carefully injecting the denser liquid from below, so that a sharp meniscus is formed. From this initial state free diffusion proceeds until an uniform concentration is reached inside the cell.

As commented earlier, nonequilibrium concentration fluctuations in this system should be described by (15), if one replaces the stationary concentration gradient ∇c_0 by $\nabla c(z,t)$, the actual concentration gradient which will depend on the time t and on the vertical coordinate z. This concentration gradient $\nabla c(z,t)$ can be calculated by solving the free-diffusion equation with a step function as initial condition. Averaging over z one obtains a time-dependent vertically averaged structure factor, which is the quantity measured in the shadowgraph experiments. The averaged structure factor has an expression similar to (24), with a time-independent amplitude $\tilde{S}^0_{\mathrm{NE}}$, but with a time-dependent roll-off wave vector $q_{\mathrm{RO}}(t)$. The details of such a calculation can be found in the corresponding literature [49].

The important point is that Brogioli et al. [70] found excellent quantitative agreement between theory and experiments, both for polymer solutions and for binary liquid mixtures. We may thus conclude that the theoretical prediction (15) for the nonequilibrium concentration fluctuations has been confirmed experimentally. This recent quantitative confirmation of the working equation for nonequilibrium concentration fluctuations for free-diffusion processes in binary liquid mixtures makes additional quantitative measurements for liquid mixtures in the case when the concentration gradient is induced by thermal diffusion even more desirable.

4 Concluding remarks

The subject of Soret-driven nonequilibrium concentration fluctuations in binary liquid systems is very interesting indeed. In this chapter we have shown how the effects of nonequilibrium concentration fluctuations on the structure factor of a binary liquid can be derived from the linearized Boussinesq equations assuming that both the thermal diffusivity D_{th} and the kinematic viscosity ν are much larger than the mutual mass diffusion coefficient D. From the experiments performed so far as reviewed in this chapter it can be said that the theory is essentially verified. Two independent research groups have obtained equivalent results by using two different experimental methods. Nevertheless it would be desirable to obtain a better quantitative agreement for binary liquid mixtures subjected to a stationary temperature gradient. A very good knowledge of the thermophysical properties of the mixtures is required for this purpose. It would also be desirable to modify the theory for the nonequilibrium concentration fluctuations to take into account boundary conditions so as to extend its validity from the $Ra < 0$, $\psi > 0$ quadrant in the stability diagram of Fig. 1 to the full region where the conductive solution is stable.

Acknowledgements

We have benefitted from a fruitful collaboration with R.W. Gammon in an earlier stage of this project. We are indebted to J.K. Platten for providing us with a copy of his publications. The research at the University of Maryland is supported by the Chemical Sciences, Geosciences and Biosciences Division of the Office of Basic Energy Sciences of the U.S. Department of Energy under Grant No. DE-FG-02-95ER-14509.

References

1. H.J.V. Tyrrell: *Diffusion and Heat Flow in Liquids.* (Butterworths, London 1961)
2. S.R. de Groot, P. Mazur: *Non-Equilibrium Thermodynamics.* (North-Holland, Amsterdam 1962)
3. D.D. Fitts: *Nonequilibrium Thermodynamics.* (McGraw-Hill, New York 1962)
4. R. Haase: *Thermodynamics of Irreversible Processes.* (Addison-Wesley, Reading MA 1969)

5. J.-L. Lin, W.L. Taylor, W.M. Rutherford: ‘Secondary Coefficients’. In: *Measurement of the Transport Properties of Fluids*, ed. by W.A. Wakeham, A. Nagashima, J.V. Sengers (Blackwell Scientific, Oxford 1991) pp. 323–387
6. R.S. Schechter, I. Prigogine, J.R. Hamm: Phys. Fluids **15**, 379 (1972)
7. R.S. Schechter, M.G. Velarde, J.K. Platten: ‘The Two-Component Bénard Problem’. In: *Advances in Chemical Physics*, Vol. 26, ed. by I. Prigogine, S.A. Rice (Wiley, New York 1974) pp. 265–301
8. J.K. Platten, G. Chavepeyer: ‘Finite Amplitude Instability in the Two-Component Bénard Problem’. In: *Advances in Chemical Physics*, Vol. 32, ed. by I. Prigogine, S. Rice (Wiley, New York 1975) pp. 281–322
9. J.K. Platten, J.C. Legros: *Convection in Liquids.* (Springer, Berlin 1984)
10. M.C. Cross, P.C. Hohenberg: Rev. Mod. Phys. **65**, 851 (1993)
11. St. Hollinger, M. Lücke: Phys. Rev. E **57**, 4238 (1998)
12. N.N. Bogoliubov: J. Phys. (USSR) **10**, 256, 265 (1946)
13. N.N. Bogoliubov: ‘Problems of a Dynamical Theory in Statistical Physics’. In: *Studies in Statistical Mechanics I, Part A*, ed. by J. de Boer, G.E. Uhlenbeck (North-Holland, Amsterdam 1962) pp. 5–118
14. J.R. Dorfman, T.R. Kirkpatrick, J.V. Sengers: Annu. Rev. Phys. Chem. **45**, 215 (1994)
15. J.V. Sengers: ‘Behavior of Viscosity and Thermal Conductivity of Fluids Near the Critical Point’. In: *Critical Phenomena*, ed. by M.S. Green, J.V. Sengers, National Bureau of Standards Miscellaneous Publication 273 (U.S. Governement Printing Office, Washington, DC 1966) pp. 165–178
16. M. Fixman: J. Chem. Phys. **47**, 2808 (1967)
17. K. Kawasaki: Ann. Phys. (NY) **61**, 1 (1970)
18. L.P. Kadanoff, J. Swift: Phys. Rev. **166**, 89 (1968)
19. P.C. Hohenberg, B.L. Halperin: Rev. Mod. Phys. **49**, 435 (1977)
20. Y. Pomeau, P. Résibois: Phys. Reports **19**, 63 (1975)
21. M.H. Ernst, E.H. Hauge, J.M.J. van Leeuwen: J. Stat. Phys. **15**, 7,23 (1976)
22. W.W. Wood: J. Stat. Phys. **57**, 675 (1989)
23. R.F. Fox: J. Phys. Chem. **86**, 2812 (1982)
24. T.R. Kirkpatrick, E.G.D. Cohen, J.R. Dorfman: Phys. Rev. A **26**, 995 (1982)
25. D. Ronis, I. Procaccia: Phys. Rev. A **26**, 1812 (1982)
26. R. Schmitz, E.G.D. Cohen: J. Stat. Phys. **40**, 431 (1985)
27. I. L’Heureux, I. Oppenheim: Physica **148A**, 503 (1988)
28. R. Schmitz: Phys. Reports **171**, 1 (1988)
29. B.M. Law, J.V. Sengers: J. Stat. Phys. **57**, 531 (1989)
30. J.V. Sengers, B.M. Law: ‘Long-range Correlations in a Fluid out of Thermal Equilibrium’. In: *Lectures on Thermodynamics and Statistical Mechanics*, ed. by M. López de Haro, C. Varea (World Scientific, Singapore 1990) pp. 201–218
31. J.V. Sengers, B.M. Law: ‘Thermal Fluctuations in a Quiescent Liquid far from Equilibrium’. In: *Nonlinear and Chaotic Phenomena in Plasmas, Solids and Fluids*, ed. by W. Rozmus, J.A. Tuszynski (World Scientific, Singapore 1991) pp. 574–581
32. B.M. Law, P.N. Segrè, R.W. Gammon, J.V. Sengers: Phys. Rev. A **41**, 816 (1990)
33. P.N. Segrè, R.W. Gammon, J.V. Sengers, B.M. Law: Phys. Rev. A **45**, 714 (1992)
34. P.N. Segrè, R.W. Gammon, J.V. Sengers: : Phys. Rev. E **47**, 1026 (1993)
35. W.B. Li, P.N. Segrè, R.W. Gammon, J.V. Sengers: Physica A **204**, 399 (1994)
36. G. Grinstein, D.-H. Lee, S. Sachdev: Phys. Rev. Lett. **64**, 1927 (1990)
37. G. Grinstein: J. Appl. Phys. **69**, 5441 (1991)

38. P.N. Segrè, R. Schmitz, J.V. Sengers: Physica A **195**, 31 (1993)
39. A. Vailati, M. Giglio: Phys. Rev. Lett. **77**, 1484 (1996)
40. A. Vailati, M. Giglio: Prog. Colloid. Polym. Sci. **104**, 76 (1997)
41. J.M. Ortiz de Zárate, R. Pérez Cordón, J.V. Sengers: Physica A **291**, 115 (2001)
42. J.M. Ortiz de Zárate, L. Muñoz Redondo: Euro. Phys. J., **21**, 135 (2001)
43. B.M. Law, J.C. Nieuwoudt: Phys. Rev. A **40**, 3880 (1989)
44. J.C. Nieuwoudt, B.M. Law: Phys. Rev. A **42**, 2003 (1990)
45. R.M. Velasco, L.S. García-Colín: J. Phys. A: Math. Gen. **24**, 1007 (1991)
46. P.N. Segrè, J.V. Sengers: Physica A **198**, 46 (1993)
47. J.V. Sengers, J.M. Ortiz de Zárate: Revista Mexicana de Física, to be published (2001)
48. R. Schmitz: Physica A **206**, 25 (1994)
49. A. Vailati, M. Giglio: Phys. Rev. E **58**, 4361 (1998)
50. W.B. Li, K.J. Zhang, J.V. Sengers, R.W. Gammon, J. M. Ortiz de Zárate: J. Chem. Phys. **112**, 9139 (2000)
51. W.B. Li, K.J. Zhang, J.V. Sengers, R.W. Gammon, J. M. Ortiz de Zárate: Phys. Rev. Lett. **81**, 5580 (1998)
52. M.G. Velarde, R.S. Schechter: Phys. Fluids **15**, 1707 (1972)
53. L.D. Landau, E.M. Lifshitz: *Fluid Mechanics*. (Addison-Wesley, Reading MA 1959)
54. D. Ronis, I. Procaccia, J. Machta: Phys. Rev. A **22**, 714 (1980)
55. S. Chandrasekhar: *Hydrodynamic and Hydromagnetic Stability*. (Clarendon, Oxford 1961)
56. R. Schmitz, E.G.D. Cohen: J. Stat. Phys. **39**, 285 (1985)
57. P.C. Hohenberg, J.B. Swift: Phys. Rev. A **46**, 4773 (1992)
58. C. Cohen, J.W.H. Sutherland, J.M. Deutch: Phys. Chem. Liquids **2**, 213 (1971)
59. W. Schöpf, W. Zimmermann: Phys. Rev. E **47**, 1739 (1993)
60. W. Hort, S.J. Linz, M. Lücke: Phys. Rev. A **45**, 3737 (1992)
61. E. Bodenschatz, W. Pesch, G. Ahlers: Annu. Rev. Fluid Mech. **32**, 709 (2000)
62. St. Hollinger, M. Lücke, H. W. Müller: Phys. Rev. E **57**, 4250 (1998)
63. M. Lücke, W. Barten, P. Büchel, F. Fütterer, St. Hollinger, Ch. Jung: ‘Pattern Formation in Binary Fluid Convection and in Systems with Throughflow’. In: *Evolution of Spontaneous Structures in Dissipative Continuous Systems*, ed. by F.H. Busse, S.C. Müller, Lecture Notes in Physics, vol. m55 (Springer, Berlin 1998) pp. 128–196
64. A. La Porta, C.M. Surko: Phys. Rev. Lett. **80**, 3759 (1998)
65. M.C. Cross, K. Kim: Phys. Rev. A **37**, 3909 (1988)
66. J.C. Legros, J.K. Platten, P.G. Poty: Phys. Fluids **15**, 1383 (1972)
67. V. De Giorgio: Phys. Rev. Lett. **41**, 1293 (1978)
68. J.S. Turner: Annu. Rev. Fluid Mech. **17**, 11 (1985)
69. A. Vailati, M. Giglio: Nature **390**, 262 (1997)
70. D. Brogioli, A. Vailati, M. Giglio: Phys. Rev. E **61**, R1 (2000); J. Phys.: Condens. Matter **12**, A39 (2000)
71. P. Cicuta, A. Vailati, M. Giglio: Phys. Rev. E **62**, 4920 (2000)
72. B.J. Berne, R. Pecora: *Dynamic Light Scattering*. (Wiley, New York 1976)
73. M. Wu, G. Ahlers, D.S. Cannell: Phys. Rev. Lett. **75**, 1743 (1995)
74. J.R. de Bruyn, E. Bodenschatz, S.W. Morris, Y. Hu, D.S. Cannell, G. Ahlers: Rev. Sci. Instrum. **67**, 2043 (1996)
75. W.B. Li, P.N. Segrè, J.V. Sengers, R.W. Gammon: J. Phys.: Condens. Matter **6**, A119 (1994)

76. W.B. Li, J.V. Sengers, R.W. Gammon, P.N. Segrè: Int. J. Thermophys. **16**, 23 (1995)
77. K.J. Zhang, M.E. Briggs, R.W. Gammon, J.V. Sengers: J. Chem. Phys. **104**, 6881 (1996)
78. J.V. Sengers, R.W. Gammon, J. M. Ortiz de Zárate: 'Thermal-Diffusion Driven Concentration Fluctuations in a Polymer Solution'. In: *Computational Studies, Nanotechnology and Solution Thermodynamics*, ed. by M. Dadmun, D. Noid, B. Sumpter, Y. Melnichenko (Kluwer, New York 2000) pp. 37–44
79. Th.G. Scholte: J. Polym. Sci. Part A-2, Polym. Phys. **8**, 841 (1970)
80. K.J. Zhang, M.E. Briggs, R.W. Gammon, J.V. Sengers, J.F. Douglas: J. Chem. Phys. **111**, 2270 (1999)

Supplementary glossary

$\boldsymbol{r}(x,y,z)$	position vector
L	finite height of the fluid layer
$\theta(\boldsymbol{r},t)$	local fluctuation of the temperature
$\Gamma(\boldsymbol{r},t)$	local fluctuation of the concentration
$w(\boldsymbol{r},t)$	local fluctuation of the z-component of velocity
∇T_0	stationary temperature gradient
∇c_0	stationary concentration gradient induced by thermal diffusion
g	gravitational acceleration constant
$\delta\mathsf{T}(\boldsymbol{r},t)$	random stress tensor
$\delta\boldsymbol{Q}(\boldsymbol{r},t)$	random heat flux
$\delta\boldsymbol{J}(\boldsymbol{r},t)$	random solute flux
Φ	scattering angle
n	refractive index
S	structure factor for Rayleigh scattering
S_{E}	structure factor in thermal equilibrium
$\tilde{S}_{\mathrm{NE}}$	normalized nonequilibrium enhancement of the structure factor
q_{RO}	gravitationally induced "roll-off" wave number (22)
s	scaled wave number (q/q_{RO})